

Risks of unavoidable impacts on forests at 1.5 °C with and without overshoot

Received: 17 January 2024

Accepted: 28 March 2025

Published online: 12 May 2025



Gregory Munday¹✉, Chris D. Jones^{1,2}✉, Norman J. Steinert^{3,4},
Camilla Mathison^{1,5}, Eleanor J. Burke¹, Chris Smith^{1,6,7},
Chris Huntingford⁸, Rebecca M. Varney⁹ & Andy J. Wiltshire^{1,9}

With global warming heading for 1.5 °C, understanding the risks of exceeding this threshold is increasingly urgent. Impacts on human and natural systems are expected to increase with further warming and some may be irreversible. Yet impacts under policy-relevant stabilization or overshoot pathways have not been well quantified. Here we report the risks of irreversible impacts on forest ecosystems, such as Amazon forest loss and high-latitude woody encroachment, under three scenarios that explore low levels of exceedance and overshoot beyond 1.5 °C. Long-term forest loss is mitigated by reducing global temperatures below 1.5 °C. The proximity of dieback risk thresholds to the bounds of the Paris Agreement global warming levels underscores the need for urgent action to mitigate climate change—and the risks of irreversible loss of an important ecosystem.

The latest Intergovernmental Panel on Climate Change (IPCC) report shows that reaching 1.5 °C of sustained global warming above pre-industrial conditions is more likely than not in the early 2030s for all commonly used scenarios of future atmospheric greenhouse gas concentrations¹. However, the future levels of global warming beyond that date are highly uncertain, being related strongly to the scenario¹. Limiting global warming to 2 °C, or even 1.5 °C above pre-industrial levels, remains a societal aspiration and was proposed as potential global policy at the 21st Conference of Parties (COP21) in Paris². Depending on the strength of policy action to reduce greenhouse gas emissions, warming could stabilize at or near 1.5 °C, temporarily overshoot and return to that level, or exceed and remain above it. Temporary temperature overshoots have been suggested as potentially safe for some components of the Earth system³. However, even if compatible with long-term global warming targets, such an approach bears considerable risks for spatially heterogeneous and potentially irreversible impacts⁴. The IPCC Synthesis Report assessed the risks of overshoot in detail and showed that both longer and higher degrees of overshoot increase the risk of potentially irreversible impacts, such as loss of ecosystems and biodiversity⁵.

The risk and magnitude of impacts due to global mean temperature overshoot and return on key forest ecosystems, such as the Amazon and boreal forests, are largely unquantified, especially those from more realistic and policy-relevant emissions scenarios. However, a number of studies have focused on tipping points, using idealized temporary overshoot trajectories. In these idealized studies, tipping points in a forest's ecosystem composition have been shown to occur at global warming levels above 2 °C, along with hysteresis in the forest's response to cooling⁶. Risk of crossing a threshold for key climate tipping elements (including the Amazon forest) has also been shown to significantly increase due to temporary overshoot⁷. Meanwhile, in the near term, a significant proportion of the Amazon is at risk of sudden, possibly irreversible, state transitions⁸. Other work has centred around biodiversity, quantifying global species' exposure⁹ and impacts on marine ecosystem habitability¹⁰ under the SSP5-3.4-OS scenario¹¹. This research also highlights the prolonged ecosystem impacts after the overshoot has peaked. The evidence provided in these simulations suggests that this is an area in need of more research across a larger range of scenarios.

The IPCC Special Report on 1.5 °C of global warming¹² identified key gaps in tools and understanding to determine the particular

¹Met Office Hadley Centre, Exeter, UK. ²School of Geographical Sciences, University of Bristol, Bristol, UK. ³NORCE Norwegian Research Centre, Bjerknes Centre for Climate Research, Bergen, Norway. ⁴CICERO Center for International Climate Research, Oslo, Norway. ⁵School of Geography, University of Leeds, Leeds, UK. ⁶International Institute for Applied Systems Analysis (IIASA), Laxenburg, Austria. ⁷Department of Water and Climate, Vrije Universiteit Brussel, Brussels, Belgium. ⁸UK Centre for Ecology and Hydrology, Wallingford, UK. ⁹Faculty of Environment, Science and Economy, University of Exeter, Exeter, UK. ✉e-mail: gregory.munday@metoffice.gov.uk; chris.d.jones@metoffice.gov.uk

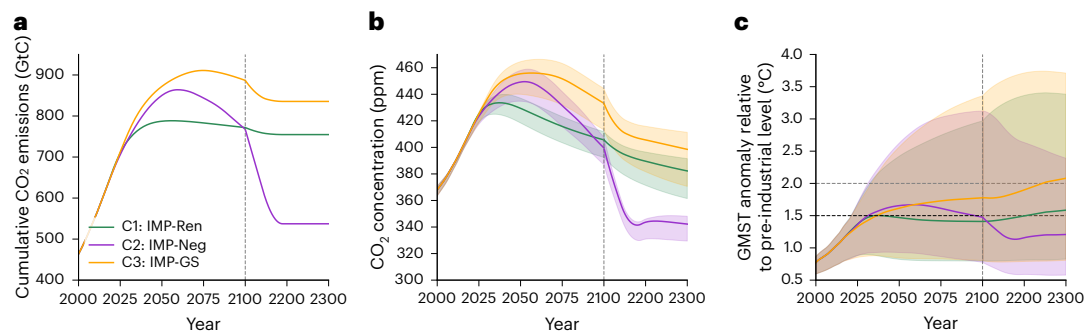


Fig. 1 | Selected IMPs. a–c, Profiles of cumulative CO₂ emissions (a), atmospheric CO₂ concentration (b) and global mean temperature change (c) calculated by the FaIR emulator, driven by emissions from C1:IMP-Ren, C2:IMP-Neg and C3:IMP-GS pathways (as labelled). The plumes in b and c represent the 0th to 100th percentile ensemble spread from FaIR, with the solid lines showing the central

ensemble member selected from mean global temperatures at year 2100. Thin horizontal lines are for warming level (compared to pre-industrial conditions) at 1.5 and 2 °C. The grey vertical lines divide the short and long-term focuses and show where FaIR's climate storylines were sampled from c.

impacts of different overshoot scenarios. There is a further requirement to create probabilistic and quantitative tools to clearly analyse the impacts between 1.5 and 2 °C of global warming. However, neither fully comprehensive Earth system models (ESMs) nor ecosystem-specific impacts models have been able to assess the implications of the most up-to-date policy scenarios. For example, Illustrative Mitigation Pathways (IMPs), some of which include overshoot trajectories, and as assessed by IPCC WGIII¹³, have only been analysed using simple climate emulators. Emulators in general simulate only global temperature and not regional changes or impacts. Instead, due to computation requirements, detailed studies with ESMs are restricted to fewer scenarios (typically those recommended by ScenarioMIP¹¹), as is the case for models in the Coupled Model Intercomparison Project (CMIP) version 6 ensemble¹⁴. Even for the earlier CMIP5 ensemble only a limited number of scenarios are investigated¹⁵. Fortunately, CMIP6 simulations with ESMs are emerging that investigate overshoot, although these tend to be more idealized calculations exploring large levels of overshoot—such as up to four times CO₂ (ref. 16) or the SSP5-3.4-OS scenario¹⁷. We aim to explore a more nuanced analysis of the additional risks during more policy-relevant, smaller overshoot scenarios. Here we find a gap between the latest policy-oriented scenario design and associated impacts analyses.

We use an emissions-to-impacts modelling framework, Probabilistic Regional Impacts from Model Patterns and Emissions (PRIME¹⁸), to bridge this gap and quantify the implications of policy-relevant overshoot scenarios for terrestrial ecosystems in a probabilistic and spatially resolved way. PRIME also allows for the quantitative assessment of long-term impacts, and here we extend the IMP scenarios to 2300 (Methods) to explore multi-century commitments of ecosystem changes. In doing so, we quantify and analyse three axes of uncertainty: societal choices through a selection of mitigation scenarios and their trajectories to 1.5 °C (and beyond), a climate emulator calibrated to sample the IPCC-assessed range of global climate sensitivities¹⁹, and a set of 34 CMIP6 patterns of climate change which sample uncertainty in regional climate response to different global warming levels. This multi-model climate space forcing in turn drives a single land surface model. In total we perform 918 simulations up to 2300.

We select three IMPs for cumulative CO₂ emissions (Fig. 1a), which generate CO₂ concentration pathways (Fig. 1b) such that the final long-term global temperature changes are trajectories near to 1.5 °C for the period from 2100 and beyond. However, their temperature pathways before eventual stabilization are very different (Fig. 1c). Specifically, our goal is to quantify differential impacts from stabilizing at or near 1.5 °C of global warming with little or no overshoot, overshooting 1.5 °C and returning by 2100, or sustained exceedance of 1.5 °C (Fig. 1c). We use these climate projections to assess the short-term (up to 2100)

and long-term (up to 2300) impacts of overshoot on two vulnerable ecosystems, focusing on ‘central estimate’ storylines to analyse the inertia of the systems’ responses to global warming. We also place an emphasis on assessing ‘high sensitivity’ storylines to describe the tail risks of overshoot associated with each of these policy-relevant pathways. We categorize safe and dangerous climatic spaces for the forests at different timescales, and look at the drivers of ecosystem net primary productivity (NPP) and irreversible forest cover loss or expansion.

Results

We analyse the impacts of the three IMPs on the resilience of Amazonian and Siberian forest ecosystems, which are known to be especially vulnerable to climate impacts^{20–23}. We focus on NPP as a measure of forest health and productivity, and simulated tree cover fraction as a longer-term integrated consequence of changes²⁴—while ecosystem health and productivity are more complex than just NPP and tree cover, further justification of these metrics is given in the Supplementary discussion. The PRIME framework¹⁸ uses the FaIR emulator²⁵ to sample the range of IPCC-assessed climate sensitivities²⁶ and calculate probabilistic global warming and CO₂ concentration profiles from emissions pathways associated with each scenario.

Our simulations span a range of CO₂ concentration and global temperature in response to CO₂ emissions in the chosen IMPs (Fig. 1). C1:IMP-Ren and C2:IMP-Neg have similar emissions at 2100, representing different policy approaches of accelerated renewable deployment and reduced emissions (C1:IMP-Ren) or reliance on negative emissions technologies later in the century (C2:IMP-Neg) to get approximately the same global warming level at 2100. Our extension to the C2 scenario includes high levels of net CO₂ removal in the twenty-second century, which consequently brings concentrations and temperatures below the C1:IMP-Ren scenario in the long term. In contrast, C3:IMP-GS has higher emissions and CO₂ throughout, and warming of around 1.8 °C by 2100. Varying levels of carbon cycle feedback sensitivities in the FaIR ensemble²⁷ account for the spread in CO₂ concentrations in these scenarios (shaded region in Fig. 1b). Carbon cycle uncertainties are small in comparison to total climate system uncertainty (shaded region in Fig. 1c and Supplementary Fig. 1), which includes the uncertainties in climate sensitivity and present-day aerosol forcing in FaIR—the key controlling factors of climate projection uncertainty²⁸.

The most likely evolution of the ecosystem response, denoted here by NPP and tree cover, varies by region and scenario (Fig. 2). In the C1:IMP-Ren and C3:IMP-GS scenarios, NPP is shown to increase with increasing temperature in both regions, which corresponds to increased tree cover. The reductions in atmospheric CO₂ (Fig. 1b) which stabilizes temperatures in these scenarios, however, results in NPP reducing in both forest ecosystems, while the tree cover continues to

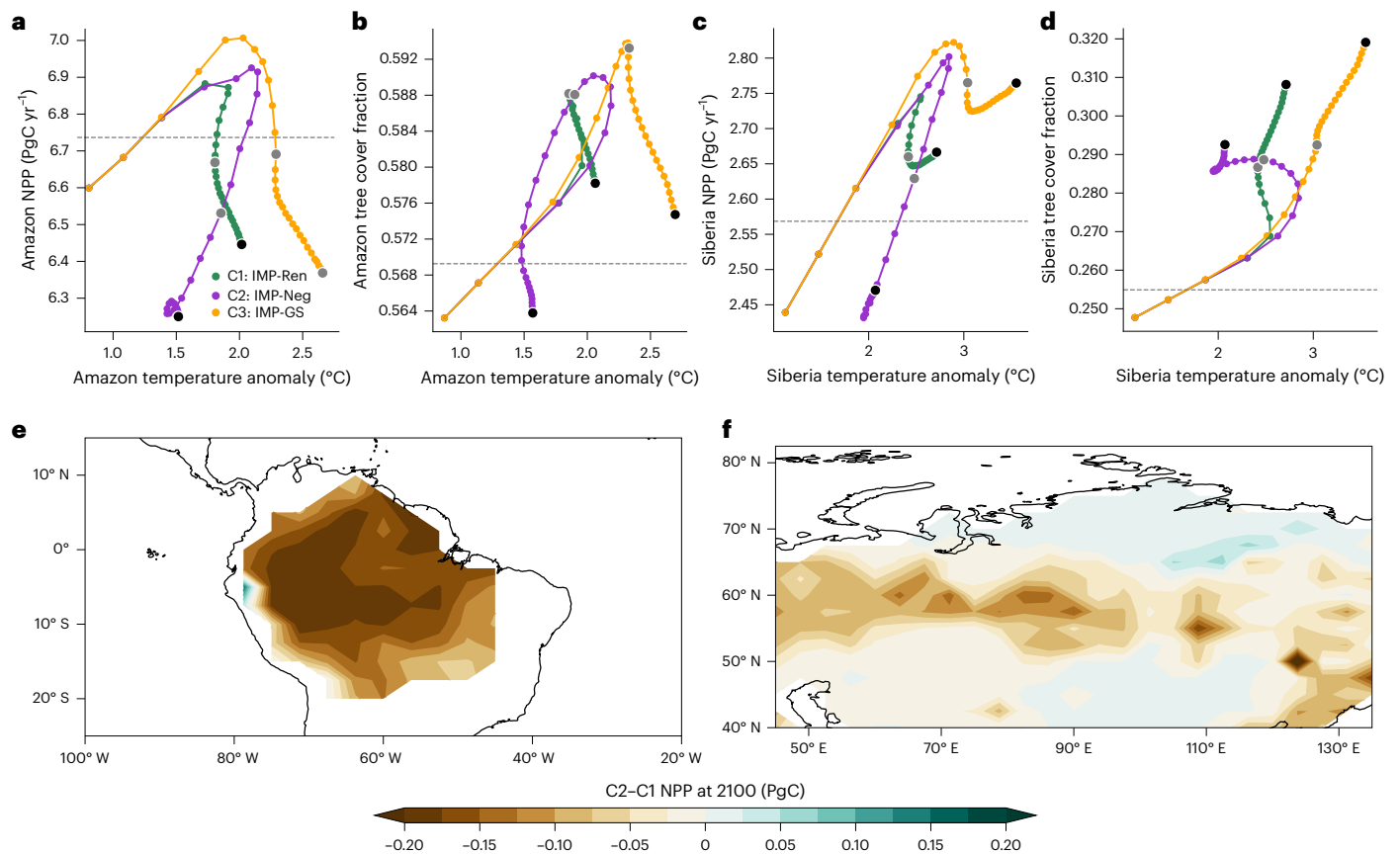


Fig. 2 | Central estimate of ecosystem response. **a–d**, The trajectory of ecosystem responses of NPP (**a,c**) and tree cover fraction (**b,d**) in the Amazonian (**a,b**) and Siberian (**c,d**) regions. Dashed grey lines denote present-day

(1995–2015) mean values. Temperatures at 2100 (grey circles) and 2300 (black circles) are shown. **e,f**, Maps showing regional differences in NPP between C2:IMP-Neg and C1:IMP-Ren at 2100 in the Amazon (**e**) and Siberia (**f**).

increase due to the inertia in its response. Amazonian NPP is shown to reduce below present-day values, resulting in a reduction in tree cover. The same reduction in tree cover is not seen in C1:IMP-Ren and C3:IMP-GS in Siberia, probably due to stabilized increased temperatures in the northern latitudes. Instead, increases in forest cover lead to woody encroachment in the region, and irreversible ecosystem composition shifts (Supplementary Figs. 2 and 3). Archer et al.²⁹ highlight that woody encroachment has significant impacts on terrestrial carbon sequestration, the hydrological cycle and biodiversity. This result also corresponds with findings from García Criado et al.³⁰, who show that woody encroachment has a positive relation to warming in the tundra biome. In the C2:IMP-Neg scenario, a greater reduction of NPP below present-day values is seen in both regions. By 2300, the increased tree cover in Siberia is limited and Amazonian tree cover is reduced below present-day. These results suggest that limiting the magnitude of overshoot is beneficial for forest health. NPP and forest cover as in Fig. 2a–d are plotted against time in Extended Data Fig. 1.

Localized impacts of differing extent of overshoot can be substantial even when global temperature has reached a similar level. Comparing the C2:IMP-Neg and C1:IMP-Ren scenarios, regional differences between small and large overshoot (Fig. 1a) can be seen in both forest ecosystems, where both IMPs arrive at similar global temperatures at 2100 (Fig. 2e,f). Despite a mean NPP difference between the C2 and C1 scenarios of 0.03 PgC in Siberia at 2100 (Fig. 2c), differences of over 12 times greater are seen regionally (Fig. 2f), and large areas of both Amazonian and Siberian forest show reduced NPP due to C2:IMP-Neg's overshoot (Fig. 1e,f). This result is consistent with Ruiz-Pérez et al.³¹, who found spatial heterogeneity in boreal forest productivity due to warming which has already occurred.

A vital part of risk assessment is beyond the central estimate response^{32,33}. PRIME allows probabilistic assessment of low-likelihood, high-impact outcomes, and here we analyse the tail risks of potentially irreversible damage to forest ecosystems. A considerable number of ensemble members show the potential for much more significant changes to both ecosystems than the central estimates (black lines in Fig. 3).

The Siberian forest is probably committed to a long-term, and possibly substantial, expansion of tree cover. Most ensemble members project a decrease in NPP (Fig. 3b), but this is relatively modest even for regional temperature increases of up to 7 °C. There is relatively little scenario dependence as NPP stays broadly within 10% of present-day values. However, all members exhibit long-term committed increases in tree cover, as NPP is above pre-industrial levels, which in extreme cases reach around 50% above present-day levels (Fig. 3d). This agrees with Pugh et al.³⁴ who saw committed boreal forest expansion and long-term carbon sink with the potential to offset carbon loss from thawing permafrost.

The Amazon forest, in contrast, is susceptible to a small but significant risk of a long-term committed and irreversible dieback (Fig. 3a,c). Some ensemble members see a decrease in NPP of 10–20% or more, which results in similar loss of forest cover. For regional warming levels above 2 °C, forest loss is potentially substantial (Extended Data Figs. 2–4). We find that, for these tail risks, the uncertainty related to FaIR's sensitivity greatly outweighs the relative differences between the scenarios, resulting in a broadly similar distribution of models with forest losses by 2100 from each scenario.

The long-term extent of Amazonian forest loss in these scenarios increases with time, with models showing increasing losses

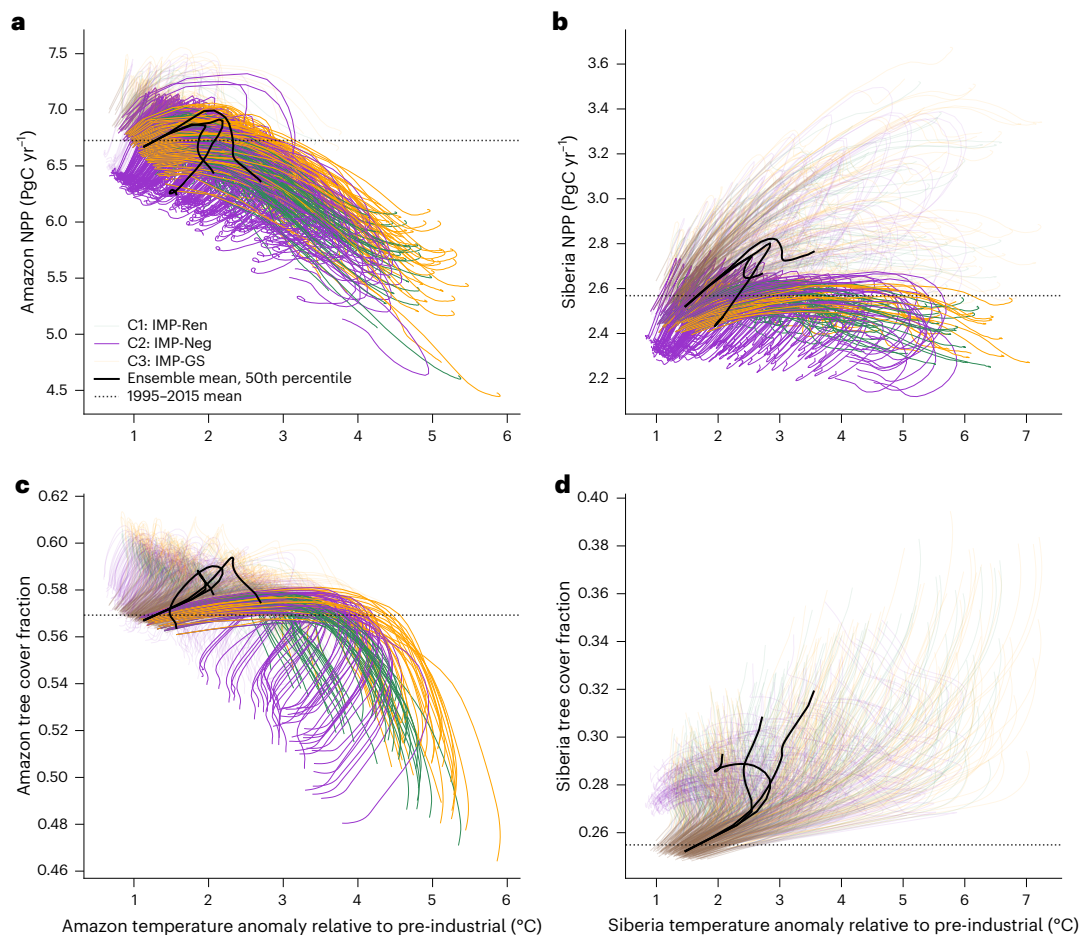


Fig. 3 | Probabilistic sampling and tail risks. a–d. The complete set of 918 NPP and tree cover fraction profiles (all climate storylines, all CMIP6 model patterns), with respect to their regional temperature anomalies. The black lines show the central estimates for each scenario. Thick lines are simulations which have

decreased below present-day levels by 2100, whereas thin lines are those which have not. Regional NPP for the Amazon (a) and Siberian forest (b); regional average tree cover fraction for the Amazon (c) and Siberia (d).

up to 2300. Under long-term stabilized global temperature characteristic of C1:IMP-Ren and C3:IMP-GS scenarios, NPP continues to decrease up to 2300, and forest fraction shows no sign of reducing its rate of loss (as indicated by the fact that the green and orange lines in Fig. 3c are vertical). In the C2:IMP-Neg overshoot scenario, the NPP has a marked behaviour; NPP values can be seen to reverse as global temperature reduces (purple lines in Fig. 3a show clear recovery) and this leads to stabilized forest cover (purple lines become horizontal in Fig. 3c).

The ecosystem response in terms of climate phase space of temperature and precipitation can provide further insight into the risk of Amazon dieback. There is a clear distinction, mainly driven by regional temperature, showing that greater levels of climate change lead to a greater chance of dieback. Although scenarios span those with wetter and drier futures, drying climate tends to also contribute to greater forest loss. If climate sensitivity at a global level led to a regional warming of 3 °C or more, then even these very low emissions scenarios have very severe impacts. Hence, there remains a low-likelihood but high-impact outcome of significant Amazon dieback even under the most aggressive mitigation policies.

Short- and long-term ‘high-risk climatic zones’ can be identified (red lines in Fig. 4), providing a range of regional average temperature and precipitation conditions for the Amazon, for which there is a significant risk of dieback. The main driver of high-risk climatic zone shifting between long- and short-term outlooks is the regional temperature. Concentrating on short-term dieback risk, we find that

58% of simulations with regional temperature greater than 2.7 °C at 2100 experience forest loss beyond present-day levels (Fig. 4a). This corresponds to a global temperature of 2.1 ± 0.5 °C (Supplementary Fig. 4). In the long term, we find that 49% of simulations with regional temperature greater than 1.7 °C at 2100 experience Amazon dieback by 2300 (Fig. 4b), corresponding to a global temperature of 1.3 ± 0.3 °C. In these high-sensitivity, high-risk futures, the Amazon experiences average diebacks of 60,000 km² by 2100 and 130,000 km² by 2300 (Extended Data Fig. 2).

The risks of Amazon dieback beyond a global temperature of 1.5 °C increase with the length of outlook. For the short term, we find that 37% of all our simulations, with regional temperatures corresponding with global temperatures greater than 1.5 °C at 2100, display some amount of dieback by 2100. This risk increases in the long term, to 55% of simulations exhibiting dieback by 2300.

Discussion

The forest response to climate change is often cited as having a risk of acting as a tipping point. In particular, there is a focus on whether this could occur for the Amazonian rainforest²². Whether this means a true tipping point, with abrupt transition to a new stable state, or simply a long-term, effectively irreversible loss of forest due to the inertia of regrowth, the risks to ecosystem functioning, carbon sinks and biodiversity are hugely important.

In determining a risk profile for forest loss for each of the pathways, we find that the uncertainty related to the sensitivities sampled

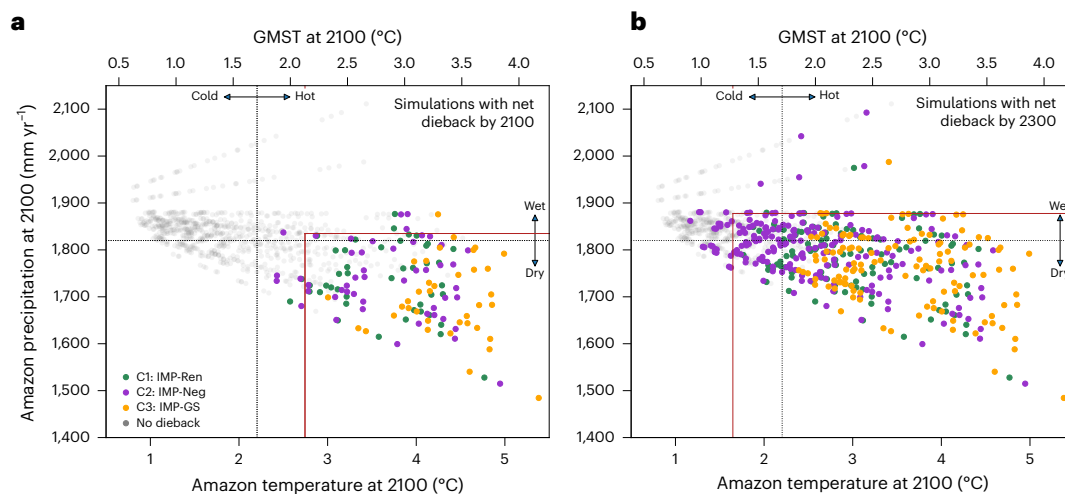


Fig. 4 | Limits of climatic drivers. Tree cover loss in the Amazon in climate phase space of temperature anomaly and precipitation relative to pre-industrial conditions. **a,b**, Simulations of tree cover declining below present-day threshold by 2100 (**a**) and 2300 (**b**) are shown in colour and the grey points show those

which did not. Regional climatic conditions are as at 2100. The grey dashed lines are the regional temperature and precipitation ensemble means at 2100. The red lines denote the 'high-risk' climatic zones, within which 95% of simulations leading to Amazon forest loss beyond present-day values, arrive.

by FaIR far outweighs that given by the differences between the selected IMPs. This is clearly illustrated by the broadly equal distribution of endpoints of all three pathways, which fall below the present-day level of forest cover in the Amazon region (Fig. 3a). There is, however, some scenario dependence of this outcome. While all three scenarios experience regional warming of 3–4 °C for their highest sensitivity members, the two which stabilize (especially C3:IMP-GS, which stabilizes at higher warming, approaching 5 °C regionally in some cases) see continued forest loss even beyond 2300, as shown by the vertical end of the lines (Fig. 3c). This indicates that stabilizing global temperature is not sufficient to stabilize the impacts of climate change. Only scenario C2:IMP-Neg, where temperature is decreasing markedly by 2300, sees the beginning of impacts stabilizing, with the curvature of the purple lines to the left (Fig. 3c). As temperature reduces, tree cover stabilizes. This highlights the long-term benefits of not stopping at net-zero: CO₂ removal, and overshoot and recovery of global temperature, can have substantial benefits in the prevention of long-term impacts. Our findings are, however, also consistent with those from Meyer et al.⁹, who found lagged and prolonged biodiversity risk exposure of over a century beyond the conclusion of overshoot in both marine and terrestrial ecosystems for SSP5-3.4-OS. Even under lower levels of overshoot, many of the C2:IMP-Neg simulations which temporarily overshoot 1.5 °C demonstrate prolonged NPP and forest loss in the Amazon for centuries afterwards (Extended Data Fig. 5).

Uncertainty in CMIP6 climate patterns also plays a role. For example, more than 50% of simulations using climate change patterns from CanESM5 and GFDL-ESM4 saw Amazon dieback, while patterns from CNRM-CM6-1 and EC-Earth3-Veg only led to dieback in the very extremes of the sensitivity. The IPCC assessment³⁵ shows a consensus of drying in the Amazon region across CMIP6 models but with substantial spread. Improved representation of changes in circulation over South America is a crucial research need, to better understand these tail risks of irreversible forest loss.

The pathway distinction matters in two aspects. First, the degree of climate change matters: higher global temperature resulting from the higher emissions in C3:IMP-GS leads to a greater risk of long-term loss compared to C1:IMP-Ren, which largely stabilizes temperature just under 1.5 °C. Second, under overshoot there is a clear benefit of returning global temperature to a lower level—even after exceeding the warming in C1:IMP-Ren, the C2:IMP-Neg pathway shows clear reductions in the long-term committed changes to forest.

Priority developments for the PRIME system first include better representation of pattern scaling for stabilization and overshoot scenarios. Second, simulating fire processes in the JULES model is a high priority, as changes in fire regime may rapidly alter ecosystem structure. Finally, species adaption is not commonly represented in global land surface models, which may alter ecosystem resilience on very long timescales.

We conclude that both of our focus ecosystems will almost certainly experience long-term committed changes, but the Amazon forest in particular is at risk of substantial loss. We delineate short- and long-term hazardous climatic spaces, where global temperature-related dieback thresholds are resolved. Our short-term dieback threshold is consistent with Armstrong McKay et al.²², who estimate an Amazon dieback tipping point global temperature range of between 2 °C and 6 °C. The threshold also aligns with that found by Albrich et al.⁶, beyond which a forest ecosystem tips into another state. However, we show that there remains a significant longer-term risk of dieback at global temperatures below this range, even under strong mitigation scenarios. Further, we determine the short- and long-term risks of Amazon forest loss associated with breaching 1.5 °C of global warming in the IMPs. These low-likelihood, high-impact risks can be ameliorated, but not removed completely, by both limiting the magnitude of warming and by aiming for temperature recovery after any temporary overshoot. Both immediate emissions reductions and long-term investment in CO₂ removal bring lasting benefits to forest health.

Online content

Any methods, additional references, Nature Portfolio reporting summaries, source data, extended data, supplementary information, acknowledgements, peer review information; details of author contributions and competing interests; and statements of data and code availability are available at <https://doi.org/10.1038/s41558-025-02327-9>.

References

1. IPCC: Summary for Policymakers. In *Climate Change 2021: The Physical Science Basis* (eds Masson-Delmotte, V. et al.) (Cambridge Univ. Press, 2021).
2. *Adoption of the Paris Agreement* FCCC/CP/2015/L.9/Rev.1 (UNFCCC, 2015).
3. Ritchie, P. D. L., Clarke, J. J., Cox, P. M. & Huntingford, C. Overshooting tipping point thresholds in a changing climate. *Nature* **592**, 517–523 (2021).

4. Bauer, N. et al. Exploring risks and benefits of overshooting a 1.5°C carbon budget over space and time. *Environ. Res. Lett.* **18**, 054015 (2023).
5. Calvin, K. et al. in *Climate Change 2023: AR6 Synthesis Report* (eds Core Writing Team, Lee H. & Romero J.) 67–89 (IPCC, 2023).
6. Albrich, K., Rammer, W. & Seidl, R. Climate change causes critical transitions and irreversible alterations of mountain forests. *Glob. Chang. Biol.* **26**, 4013–4027 (2020).
7. Wunderling, N. et al. Global warming overshoots increase risks of climate tipping cascades in a network model. *Nat. Clim. Change* **13**, 75–82 (2023).
8. Flores, B. M. et al. Critical transitions in the Amazon forest system. *Nature* **626**, 555–564 (2024).
9. Meyer, A. L., Bentley, J., Odoulami, R. C., Pigot, A. L. & Trisos, C. H. Risks to biodiversity from temperature overshoot pathways. *Phil. Trans. R. Soc. B* **377**, 20210394 (2022).
10. Santana-Falcón, Y. et al. Irreversible loss in marine ecosystem habitability after a temperature overshoot. *Commun. Earth Environ.* **4**, 343 (2023).
11. O'Neill, B. C. et al. The Scenario Model Intercomparison Project (ScenarioMIP) for CMIP6. *Geosci. Model Dev.* **9**, 3461–3482 (2016).
12. Hoegh-Guldberg, O. et al. in *Special Report on Global Warming of 1.5°C* (eds Masson-Delmotte, V. et al.) Ch. 3 (IPCC, WMO, 2018).
13. IPCC: Summary for Policymakers. In *Climate Change 2022: Mitigation of Climate Change* (eds Shukla, P. R. et al.) (Cambridge Univ. Press, 2022).
14. Eyring, V. et al. Overview of the Coupled Model Intercomparison Project Phase 6 (CMIP6) experimental design and organization. *Geosci. Model Dev.* **9**, 1937–1958 (2016).
15. Frieler, K. et al. Assessing the impacts of 1.5°C global warming – simulation protocol of the Inter-Sectoral Impact Model Intercomparison Project (ISI-MIP2b). *Geosci. Model Dev.* <https://doi.org/10.5194/gmd-10-4321-2017> (2017).
16. Keller, D. P. et al. The Carbon Dioxide Removal Model Intercomparison Project (CDRMIP): rationale and experimental protocol for CMIP6. *Geosci. Model Dev.* <https://doi.org/10.5194/gmd-11-1133-2018> (2018).
17. Koven, C. D. et al. Multi-century dynamics of the climate and carbon cycle under both high and net negative emissions scenarios. *Earth Syst. Dyn.* **13**, 885–909 (2022).
18. Mathison, C. et al. A rapid-application emissions-to-impacts tool for scenario assessment: Probabilistic Regional Impacts from Model patterns and Emissions (PRIME). *Geosci. Model Dev.* **18**, 1785–1808 (2025).
19. Smith, C. et al. in *The Earth's Energy Budget, Climate Feedbacks, and Climate Sensitivity Supplementary Material* (eds Masson-Delmotte, V. et al.) 9–14 (IPCC, 2021).
20. IPCC: Summary for policymakers. In *Climate Change 2022: Impacts, Adaptation and Vulnerability* (eds Pörtner, H.-O. et al.) <https://doi.org/10.1017/9781009325844.001> (Cambridge Univ. Press, 2022).
21. Jones, C., Lowe, J., Liddicoat, S. & Betts, R. Committed terrestrial ecosystem changes due to climate change. *Nat. Geosci.* <https://doi.org/10.1038/ngeo555> (2009).
22. Armstrong McKay, D. I. et al. Exceeding 1.5°C global warming could trigger multiple climate tipping points. *Science* **377**, eabn7950 (2022).
23. Jones, C., Liddicoat, S. & Lowe, J. Role of terrestrial ecosystems in determining CO₂ stabilization and recovery behaviour. *Tellus B* <https://doi.org/10.1111/j.1600-0889.2010.00490.x> (2010).
24. Taelman, S. E., Schaubroeck, T., De Meester, S., Boone, L. & Dewulf, J. Accounting for land use in life cycle assessment: the value of NPP as a proxy indicator to assess land use impacts on ecosystems. *Sci. Total Environ.* **550**, 143–156 (2016).
25. Smith, C. J. et al. FAIR v1.3: a simple emissions-based impulse response and carbon cycle model. *Geosci. Model Dev.* **11**, 2273–2297 (2018).
26. Forster, P. et al. in *Climate Change 2021: The Physical Science Basis* (eds Masson-Delmotte, V. et al.) 923–1054 (IPCC, Cambridge Univ. Press, 2021).
27. Leach, N. J. et al. FaIR v2.0.0: a generalized impulse response model for climate uncertainty and future scenario exploration. *Geosci. Model Dev.* **14**, 3007–3036 (2021).
28. Smith, C. J. et al. Current fossil fuel infrastructure does not yet commit us to 1.5°C warming. *Nat. Commun.* **10**, 101 (2019).
29. Archer, S. R. et al. in *Rangeland Systems* 1st edn (ed. Briske, D. A.) Ch. 2 (Springer Cham, 2017).
30. García Criado, M., Myers-Smith, I. H., Bjorkman, A. D., Lehmann, C. E. & Stevens, N. Woody plant encroachment intensifies under climate change across tundra and savanna biomes. *Glob. Ecol. Biogeogr.* **29**, 925–943 (2020).
31. Ruiz-Pérez, G. & Vico, G. Effects of temperature and water availability on northern European boreal forests. *Front. For. Glob. Change* **3**, 34 (2020).
32. Xu, Y. & Ramanathan, V. Well below 2°C: mitigation strategies for avoiding dangerous to catastrophic climate changes. *Proc. Natl Acad. Sci. USA* **114**, 10315–10323 (2017).
33. Sutton, R. T. ESD ideas: a simple proposal to improve the contribution of IPCC WGI to the assessment and communication of climate change risks. *Earth Syst. Dyn.* **9**, 1155–1158 (2018).
34. Pugh, T. A. M. et al. A large committed long-term sink of carbon due to vegetation dynamics. *Earth's Future* <https://doi.org/10.1029/2018EF000935> (2018).
35. Lee, J.-Y. et al. in *Climate Change 2021: The Physical Science Basis* (eds Masson-Delmotte, V. et al.) Ch. 4 (IPCC, Cambridge Univ. Press, 2021).

Publisher's note Springer Nature remains neutral with regard to jurisdictional claims in published maps and institutional affiliations.

Open Access This article is licensed under a Creative Commons Attribution 4.0 International License, which permits use, sharing, adaptation, distribution and reproduction in any medium or format, as long as you give appropriate credit to the original author(s) and the source, provide a link to the Creative Commons licence, and indicate if changes were made. The images or other third party material in this article are included in the article's Creative Commons licence, unless indicated otherwise in a credit line to the material. If material is not included in the article's Creative Commons licence and your intended use is not permitted by statutory regulation or exceeds the permitted use, you will need to obtain permission directly from the copyright holder. To view a copy of this licence, visit <http://creativecommons.org/licenses/by/4.0/>.

© Crown 2025

Methods

Scenario selection

We evaluate three of the seven IMPs, which are socioeconomic scenarios derived from integrated assessment models. The three selected IMPs were chosen to give a broad and representative view into differing potential future climate scenarios. The IMPs were used in the IPCC's Sixth Assessment Report Working Group 3³⁶ to demonstrate a range of techno-socio-economic solutions to meeting the 1.5 °C and 2 °C Paris Agreement targets, but have not previously been run in ESMs.

IPCC WG3 classified emissions scenarios into eight categories depending on their peak and end-of-century temperature. The lowest three C1, C2 and C3 scenario groupings can be interpreted as being broadly consistent with 1.5 °C (C1) and well-below 2 °C (C2 and C3) thresholds of the Paris Agreement, though this is not strictly defined³⁷. C1 refers to scenarios which peak below 1.5 °C with a probability of at least 33%, and are below 1.5 °C in 2100 with a probability of at least 50%. Median peak warming, therefore, may temporarily exceed 1.5 °C, allowing for a small overshoot, typically less than 0.1 °C. C2 scenarios have peak warming exceeding 1.5 °C with a probability of more than 33%, but still return to less than 1.5 °C in 2100 with greater than 50% chance, hence having a larger overshoot of peak warming typically in the 0.1–0.3 °C range. C2 scenarios are sometimes referred to as '1.5 °C with high overshoot'. C3 scenarios do not return below 1.5 °C in the median before 2100 but remain 'well below' 2 °C throughout the twenty-first century, interpreted as at least 67% chance of not exceeding 2 °C and typically with median warming not exceeding 1.85 °C. References to probabilities relate to these scenarios being run with a simple climate model hundreds of times, perturbing parametric uncertainty in future climate change. Scenario classification in AR6 was performed using MAGICC³⁸. We retain the original IPCC classifications in this paper though report our results using FaIR, resulting in marginally cooler projections.

From the seven IMPs, we select one representative scenario per category for the headline results in this paper. From C1 we use IMP-Ren (REMIND-MAGPIE 2.1-4.3 DeepElec_SSP2_HighRE_Budg900)³⁹ and from C3 we use IMP-GS (WITCH 5.0 CO_Bridge)⁴⁰. The C1:IMP-Ren scenario is a low emissions scenario, chosen as our default scenario given its achievement of 1.5 °C global warming with little overshoot, enabled by steep reductions and replacement of fossil fuels with renewables. C3:IMP-GS prescribes a gradual strengthening of combinations of renewables uptake and CO₂ removal. For C2 there is a sole representative in the IMPs: IMP-Neg (COFFEE 1.1 EN_NPi2020_400f_lowBECCS), a scenario with a large scale-up of negative CO₂ emissions in the second half of the century⁴¹. IMP-Neg is technically a C3 scenario in AR6, though it is characteristic of C2 scenarios²⁹ and its warming profile in FaIR satisfies the C2 definition.

PRIME

We use the PRIME framework¹⁸ to examine 918 potential futures (three IMPs, nine climate storylines and 34 CMIP6 model patterns). We use FaIR v.1.6.2, the reduced complexity climate model²⁵, to produce CO₂ concentration profiles and global mean temperature projections driven by IMP emissions data, generating 2,237 ensemble members¹⁹ per IMP. Nine ensemble members were subsequently subsampled from the original 2,237 from the C1:IMP-Ren scenario, with those ensemble members being used consistently in all three IMPs, enabling a pairwise comparison between members in different scenarios (Supplementary Fig. 5). Therefore, each scenario member relates to a particular climate storyline. The nine ensemble members represent the 0th, 1st, 5th, 25th, 50th, 75th, 95th, 99th and 100th percentiles of global mean temperature response from the 2,237-member FaIR ensemble at 2100 (Supplementary Fig. 1 and Table 1). This approach is in contrast to many probabilistic projections of future climate change, which take statistics across the ensemble at each time point. Hence, we refer to the 'low sensitivity', 'central' and 'high sensitivity' ensemble members to represent the storylines tied to the 5th or below, 50th and 95th or above percentiles in 2100, rather than, for example, the 'ensemble median' for the 50th.

The global temperature profiles produced by FaIR were used to scale monthly aggregated climate patterns derived from 34 CMIP6 (Eyring et al.¹⁴) ESMs (Supplementary Table 2), encapsulating the range of uncertainty and enabling the emulation of the CMIP6 ensemble response to the IMPs' associated global warming projections. We follow a proven pattern-scaling methodology^{42,43}, further detailed and evaluated in Mathison et al.¹⁸, and use the climate patterns to drive a land surface model (JULES) to recover terrestrial ecosystem impacts.

The Joint UK Land Environment Simulator Earth System (JULES^{44–46}) is a community land surface model that can be used in either standalone mode or coupled with the UK Earth System Model⁴⁷. Here we use the JULES-ES configuration⁴⁸, which includes a representation of both dynamic vegetation and nitrogen limitation. We do not include any land use change to focus on the ecosystems' response to climate. Fire modelling is in its infancy and not included in our current set-up, but changes in fire regime are important⁴⁹ and possible amplifiers of abrupt change. We recommend its inclusion in future studies towards IPCC AR7.

JULES was driven by temporally and regionally downscaled hourly weather data. This downscaled time series was reconstructed by superimposing the local change in the meteorology caused by the global mean temperature change multiplied by the climate patterns on an observed climatology derived for the period 1901–1930 from the GSWP3-W5E5 dataset from the ISIMIP3a project⁵⁰.

These global pathways are combined with spatial patterns of climate change for temperature, rainfall, humidity, radiation, wind speed and pressure from CMIP6 ESMs. These patterns are used to run the land surface model JULES to simulate the impacts on global ecosystems. A validation of PRIME using the SSP-RCPs, for which ESM output is available, is demonstrated by Mathison et al.¹⁸.

IMP extensions

We extend the IMPs examined in this study from 2100 to 2300 following the methodology designed by Meinhausen et al.⁵¹, which was also used previously to extend the shared socioeconomic pathway simulations. In these extensions, the emissions before 2100 remain unchanged and are identical to those in the AR6 WGIII report for the scenarios presented. The approach for fossil CO₂ emissions post 2100 depends on if they are positive or negative in 2100. If positive, the fossil CO₂ emissions are ramped down to zero by 2250, if negative they are held constant at 2100 levels to 2140, at which point they are brought back to zero by 2190, reflecting the assumption that negative emissions cannot continue indefinitely. Non-CO₂ emissions from fossil and industry (always positive) are ramped down linearly from their 2100 levels to zero in 2250. Agriculture, forestry and other land use CO₂ emissions (whether net positive or net negative) are ramped linearly from their 2100 levels to zero in 2150, while non-CO₂ land use emissions are held constant at 2100 levels. This is most consistent with the assumption of a constant land use between 2100–2300, which represents a more plausible future given that food production will continue, and this will result in some emissions, for example, N₂O and CH₄.

We use the methods described to analyse two vulnerable regions: the Amazon and a region of boreal forest in Siberia (45–80° N, 45–135° E) (Supplementary Fig. 6). The Amazon region boundary was defined using data from the MapBiomass Amazonia Project⁵². For the comparison of end-of-century and long-term predictions for ecosystem impacts against present-day conditions, we calculate a 1995–2015 reference period. This is constructed by evaluating the means of simulated outputs resulting from inputs of all available CMIP6 patterns and the three IMPs, driven using FaIR's central ensemble member. These reference periods are used as reference levels for tree cover fraction and NPP when we assess risks of irreversible impacts or forest loss.

Data availability

Model output from FaIR and JULES used in this paper are available via Zenodo at <https://doi.org/10.5281/zenodo.15097561> (ref. 53).

Calibration data for FaIR v1.6.2 are available at <https://doi.org/10.5281/zenodo.6601980> (ref. 54). The Illustrative Mitigation Pathways emissions data are available from the IPCC AR6 Scenarios Database, hosted at <https://data.ece.iiasa.ac.at/ar6/> (ref. 55) and CMIP6 data are available at <https://esgf-node.llnl.gov/search/cmip6/> (ref. 14). The Amazon region boundary was selected using data from the MapBiomass Amazonia Project (ref. 52).

Code availability

The code for analysis and plotting of the PRIME outputs is available with the models' output data via Zenodo at <https://doi.org/10.5281/zenodo.15097561> (ref. 53). FaIR v1.6.2 is available from the Python Package Index at <https://pypi.org/project/fair/1.6.2/>, via GitHub at <https://github.com/OMS-NetZero/FAIR/tree/v1.6.2> and via Zenodo at <https://doi.org/10.5281/zenodo.4465032> (ref. 56). The code calculating the climate patterns used to drive JULES is available in ESMValTool via Zenodo at <https://doi.org/10.5281/zenodo.12654299> (ref. 57) and it downloads the required model data on the fly. Access to the JULES code used in this study is available on request from the corresponding authors.

References

36. Lecocq, F. et al. in *Climate Change 2022: Mitigation of Climate Change* (eds Shukla, P. R. et al.) Ch. 4 (IPCC, Cambridge Univ. Press, 2022).
37. Guivarch, C. et al. in *Climate Change 2022: Mitigation of Climate Change* (eds Shukla, P. R. et al.) 1841–1908 (IPCC, Cambridge Univ. Press, 2022).
38. Meinshausen, M. et al. The RCP greenhouse gas concentrations and their extensions from 1765 to 2300. *Clim. Change* <https://doi.org/10.1007/s10584-011-0156-z> (2011).
39. Luderer, G. et al. Impact of declining renewable energy costs on electrification in low-emission scenarios. *Nat. Energy* **7**, 32–42 (2021).
40. van Soest, H. L. et al. Global roll-out of comprehensive policy measures may aid in bridging emissions gap. *Nat. Commun.* **12**, 6419 (2021).
41. Riahi, K. et al. Cost and attainability of meeting stringent climate targets without overshoot. *Nat. Clim. Change* **11**, 1063–1069 (2021).
42. Huntingford, C. & Cox, P. M. An analogue model to derive additional climate change scenarios from existing GCM simulations. *Clim. Dyn.* **16**, 575–586 (2000).
43. Wells, C. D., Jackson, L. S., Maycock, A. C. & Forster, P. M. Understanding pattern scaling errors across a range of emissions pathways. *Earth Syst. Dyn.* **14**, 817–834 (2023).
44. Best, M. J. et al. The Joint UK Land Environment Simulator (JULES), model description – part 1: energy and water fluxes. *Geosci. Model Dev.* **4**, 677–699 (2011).
45. Clark, D. B. et al. The Joint UK Land Environment Simulator (JULES), model description – part 2: carbon fluxes and vegetation. *Geosci. Model Dev. Discuss.* <https://doi.org/10.5194/gmdd-4-641-2011> (2011).
46. Wiltshire, A. J. et al. JULES-CN: a coupled terrestrial carbon–nitrogen scheme (JULES vn5.1). *Geosci. Model Dev.* **14**, 2161–2186 (2021).
47. Sellar, A. A. et al. UKESM1: description and evaluation of the UK Earth System Model. *J. Adv. Model. Earth Syst.* <https://doi.org/10.1029/2019MS001739> (2019).
48. Mathison, C. et al. Description and evaluation of the JULES-ES set-up for ISIMIP2b. *Geosci. Model Dev.* **16**, 4249–4264 (2023).
49. Burton, C. et al. South American fires and their impacts on ecosystems increase with continued emissions. *Clim. Resil. Sustain.* **1**, e8 (2021).
50. Frieler, K. et al. Scenario setup and forcing data for impact model evaluation and impact attribution within the third round of the Inter-Sectoral Impact Model Intercomparison Project (ISIMIP3a). *Geosci. Model Dev.* **17**, 1–51 (2024).
51. Meinshausen, M. et al. The shared socio-economic pathway (SSP) greenhouse gas concentrations and their extensions to 2500. *Geosci. Model Dev.* **13**, 3571–3605 (2020).
52. MapBiomass Amazonia Project – Collection 6 of the Annual Land Cover & Land Use Map Series (MapBiomass, accessed 16 April 2025); <https://plataforma.amazonia.mapbiomas.org>
53. Munday, G. et al. Code for 'risks of unavoidable impacts on forests at 1.5C with and without overshoot.' (v4) Zenodo <https://doi.org/10.5281/zenodo.15097561> (2025).
54. Smith, C. Fair v1.6.2 calibrated and constrained parameter set. Zenodo <https://doi.org/10.5281/zenodo.6601980> (2022).
55. Byers, E. et al. AR6 Scenarios Database Hosted by IIASA. (International Institute for Applied Systems Analysis, accessed 16 April 2025).
56. C. Smith, Z. Nicholls, & R. Gieseke. OMS-NetZero/FAIR: updates to ozone forcing (v1.6.2). Zenodo <https://doi.org/10.5281/zenodo.4465032> (2021).
57. Andela, B. et al. ESMValTool. Zenodo <https://doi.org/10.5281/zenodo.12654299> (2024).

Acknowledgements

This work was supported by the Joint UK BEIS/Defra Met Office Hadley Centre Climate Programme (GA01101), the Newton Fund through the Met Office Climate Science for Service Partnership Brazil (CSSP Brazil), the Natural Environment Research Council (NE/T009381/1) and the European Union's Horizon 2020 research and innovation programme under grant agreement no. 101003536 (ESM2025—Earth System Models for the Future) and 101081661 (WorldTrans). N.J.S. acknowledges funding from the Research Council of Norway (project IMPOSE, grant no. 294930), ESM2025, as well as funding from the Norwegian Research Centre AS (NORCE). C.H. received support under national capability funding as part of the Natural Environment Research Council UK-SCAPE programme (award no. NE/R016429/1). R.M.V. was supported by the European Research Council's Climate–Carbon Interactions in the Current Century project (4C; grant no. 821003).

Author contributions

C.D.J. and G.M. conceived and designed the study with input from N.J.S. G.M. performed the numerical analysis with contributions from N.J.S. Simulations were performed by C.M., C.S. and E.J.B. C.H. and R.M.V. contributed to discussions, wrote and revised sections of the paper. A.J.W. created the joint distribution plot in the Supplementary Information. All authors discussed and interpreted results, drew conclusions and wrote the paper.

Competing interests

The authors declare no competing interests.

Additional information

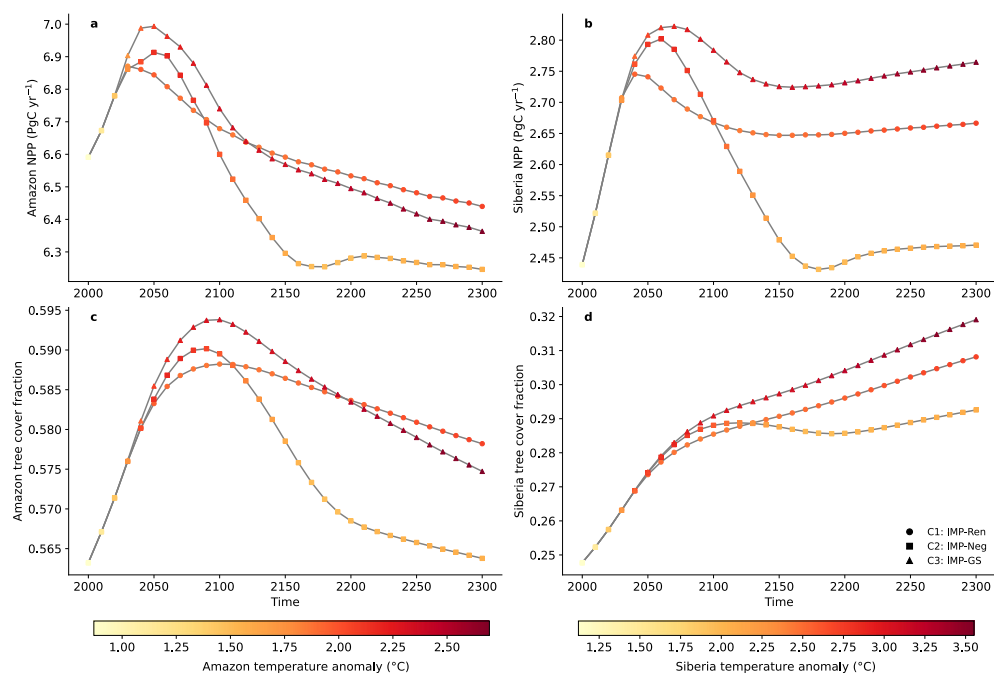
Extended data is available for this paper at <https://doi.org/10.1038/s41558-025-02327-9>.

Supplementary information The online version contains supplementary material available at <https://doi.org/10.1038/s41558-025-02327-9>.

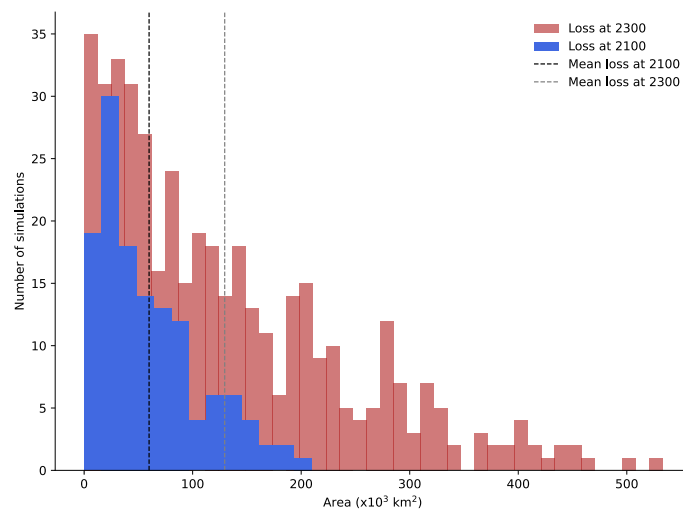
Correspondence and requests for materials should be addressed to Gregory Munday or Chris D. Jones.

Peer review information *Nature Climate Change* thanks Silvia Caldararu, Andreas Luiz Schwarz Meyer and the other, anonymous, reviewer(s) for their contribution to the peer review of this work.

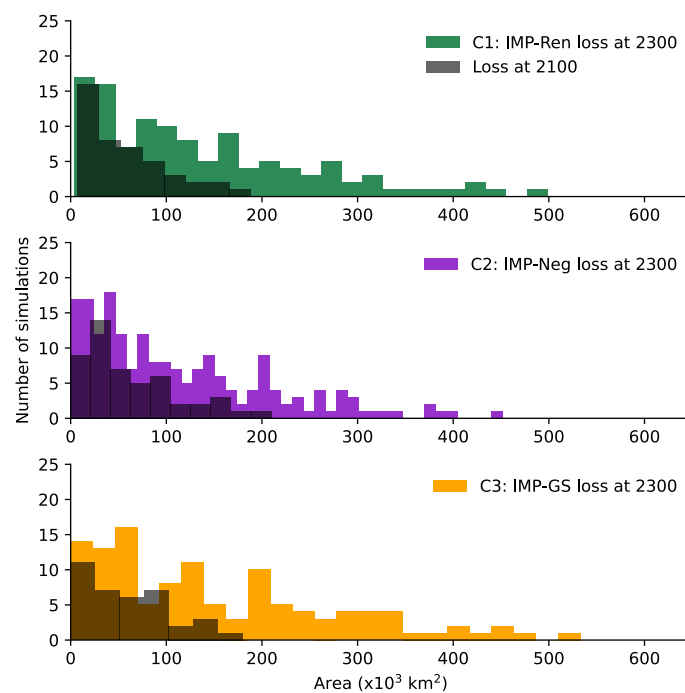
Reprints and permissions information is available at www.nature.com/reprints.



Extended Data Fig. 1 | Ecosystem impacts over time. Central estimate-driven simulations of regionally averaged net primary productivity (NPP) and tree cover fraction against time for the Amazon **a,c** and Siberia **b,d** for each of our selected Illustrative Mitigation Pathways. The temperature anomaly for each of the regions is shown by colour.

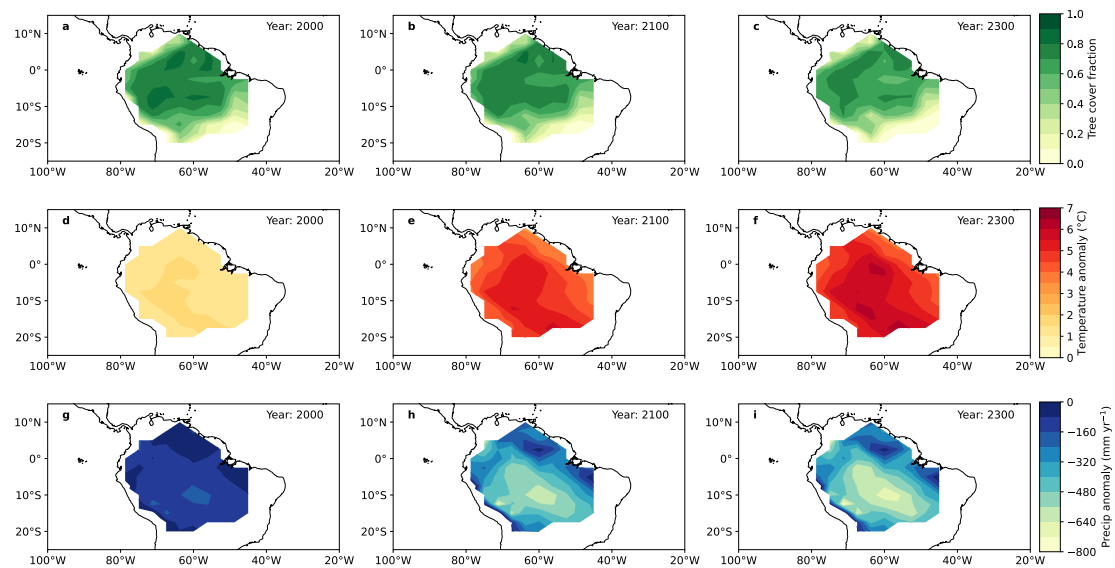


Extended Data Fig. 2 | Amazon forest loss distributions. Distributions of the area of Amazon forest cover lost under all selected Illustrative Mitigation Pathways, all ensemble members and model patterns at 2100 and 2300. Vertical lines designate mean losses of 65,000 km^2 at 2100 and 146,000 km^2 at 2300. Only those simulations which show forest loss by each time period are displayed.

**Extended Data Fig. 3 | Pathway-specific Amazon forest loss distributions.**

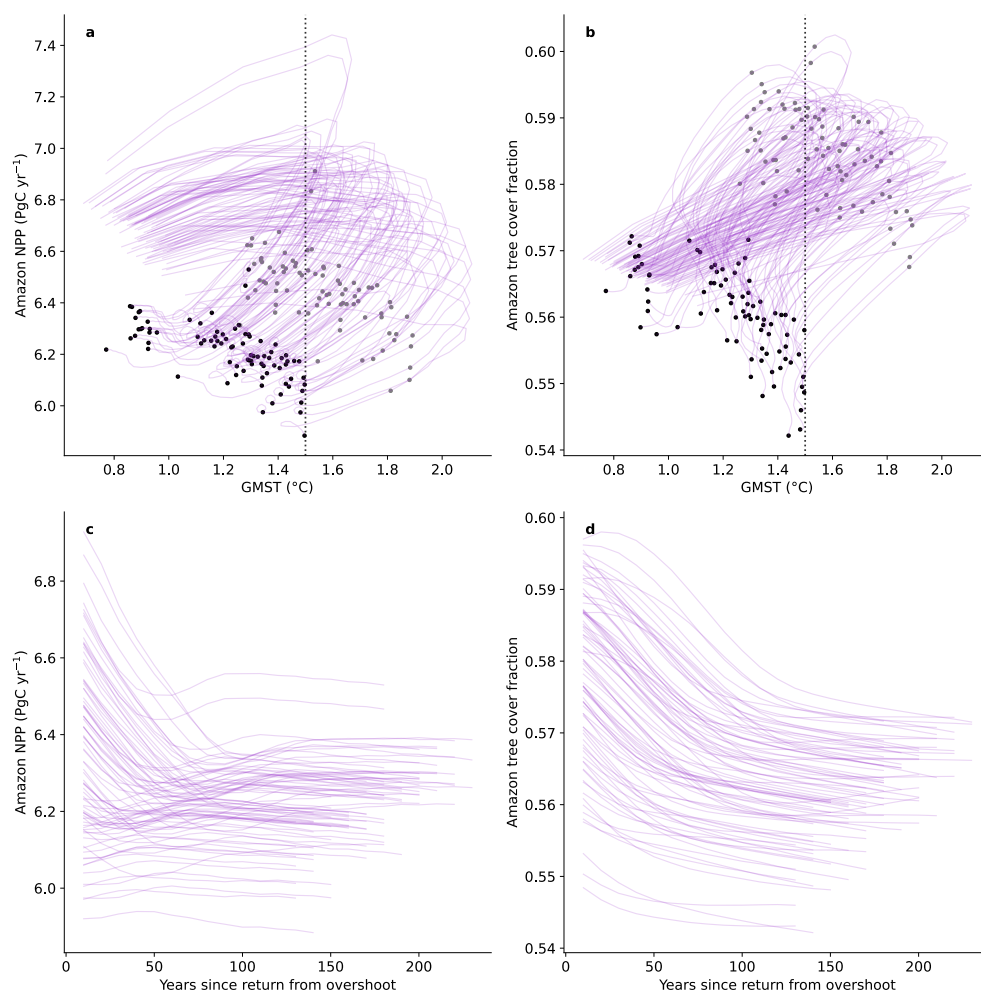
Amazon forest cover loss distributions separated for each scenario at 2100 and 2300. Only those simulations displaying forest loss by each period are shown.

The similarity in these loss distributions reinforce our findings that forest loss risk is mainly driven by sensitivities sampled by the FaIR climate model rather than by scenario, and by proxy our different climate storylines.



Extended Data Fig. 4 | Maps of forest cover loss in the Amazon. Simulations of **a,b,c** tree cover fraction, **d,e,f** near-surface air temperature and **g,h,i** precipitation, driven by the S99 climate storyline and patterns selected from the

GFDL-ESM4 earth system model. These maps illustrate the evolution of regional ecosystem and climate change, and spatial heterogeneity of forest loss in the Amazon with its key drivers.



Extended Data Fig. 5 | Prolonged impacts after overshoot. C2:IMP-Neg simulations of **a** Amazon NPP, **b** tree cover fraction against global mean surface temperature, **c** Amazon NPP and **d** tree cover fraction versus the number of years since the end of overshoot. Only simulations whose global temperature trajectories returned below 1.5°C are included here. In **a**, **b** the grey points

designate the year 2100, and the black points show 2300. These panels indicate that in simulations where global temperature stabilizes or continues to decrease post-overshoot, Amazon forest health and cover fraction show protracted decline.